

Study of Plasma Current Decay in the Initial Phase of High Poloidal Beta Disruptions in JT-60U

Yoshihide SHIBATA, Kiyomasa WATANABE¹⁾, Noriyasu OHNO, Masaaki OKAMOTO²⁾, Akihiko ISAYAMA³⁾, Kenichi KURIHARA³⁾, Naoyuki OYAMA³⁾, Tomohide NAKANO³⁾, Yasunori KAWANO³⁾, Go MATSUNAGA³⁾, Yutaka KAMADA³⁾ and Masayoshi SUGIHARA⁴⁾

*Department of Energy Engineering and Science, Graduate School of Engineering,
Nagoya University, Nagoya 464-8603, Japan*

¹⁾*National Institute for Fusion Science, Toki 509-5292, Japan*

²⁾*Ishikawa National College of Technology, Ishikawa 929-0392, Japan*

³⁾*Japan Atomic Energy Agency, Naka 311-0193, Japan*

⁴⁾*ITER Organization, Cadarache 13076 France*

(Received 31 May 2011 / Accepted 27 August 2011)

In order to validate some current decay models during the current quench, the plasma current decay time was studied using the experimental plasma resistance and inductance in high poloidal beta, β_p , disruptions in JT-60U. The plasma resistance and inductance were evaluated from an equilibrium calculation code and the measurement value of a magnetic sensor, the electron temperature evaluated by using ECE measurement and the electron density measured by FIR interferometer. In high β_p disruptions, it was found that the electron temperature at the plasma center just after current quench starts was approximately 1-4 keV under almost the same current decay time observed during the initial phase of current quench. This result indicates that the electron temperature itself plays no major role in the determination of the current decay time in the initial phase of current quench. Moreover, the current decay time predicted by a modified L/R model [Y. Shibata *et al.*, Nucl. Fusion **50**, 025015 (2010)], in which the time derivative of plasma inductance was considered, was in good agreement with the experimental current decay time, while the values obtained from the conventional L/R model were two orders of magnitude larger than the experimental results.

© 2011 The Japan Society of Plasma Science and Nuclear Fusion Research

Keywords: current decay model, disruption, high β_p plasma discharge, plasma inductance, poloidal beta

DOI: 10.1585/pfr.6.1302136

A precise prediction of plasma current decay time, τ , is important for estimating the electromagnetic forces acting on the vacuum vessel and the in-vessel components during the tokamak disruption. The so-called “ L/R model” often used to predict the current decay time in ITER [1] is based on a simple series circuit that considers the plasma resistance R_p and inductance L_p , which are constant in time. In the “ L/R model”, the current decay time is represented by $\tau_{L/R} = L_p/R_p$. If the plasma resistivity is defined by Spitzer resistivity [2], the current decay time is mainly determined by the electron temperature T_e and effective charge Z_{eff} . Thus, the area-normalized τ in current quench was intensely investigated among medium- and large-size tokamaks [1] and spherical torus [3] and the results are summarized as a database up to now. In the database in Ref. [1], the lower bound of the area-normalized τ is $1.7 \times 10^{-3} \text{s/m}^2$, which is used as the criterion value for ITER design. However, a systematic research on the relationship between the current decay time during disruption and the measurement value of the plasma inductance and

resistance has rarely been conducted thus far.

In the 2008 JT-60U experimental campaign, the current decay in the radiative disruption generated by a massive neon gas-puff was investigated [4]. In Ref. [4], the current decay during the initial phase of current quench, which is the time region in which plasma current decays to 90% of that just after the start of current quench, was investigated through a comparative analysis with the time evolution of plasma resistance and inductance that were evaluated by the measurement value of a magnetic sensor and the electron temperature. We focused on the initial phase of current quench because plasma inductance and resistance measurements are very noisy in other phase. In addition, the electromagnetic forces are proportional to the amplitude of plasma current because electromagnetic forces are proportional to $dI_p/dt \sim I_p/\tau$. It was found that the experimental current decay time, τ_{exp} , did not match that predicted by the “ L/R model” in the initial phase of current quench [4]. The conventional “ L/R model” is obtained under the assumption that plasma inductance and resistance are constant during the current quench phase.

author's e-mail: y-shibata@ees.nagoya-u.ac.jp

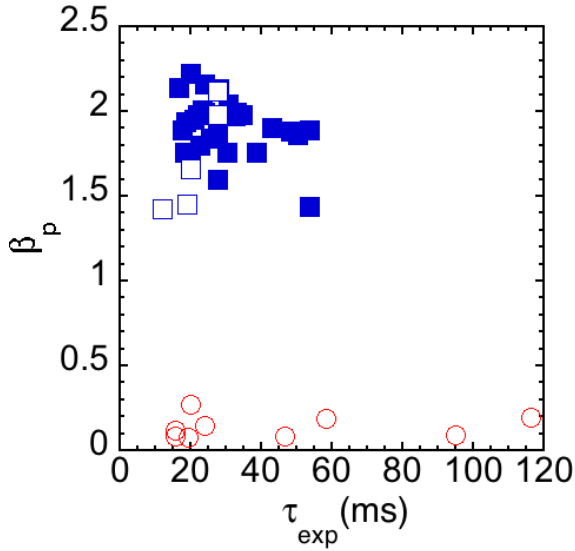


Fig. 1 Poloidal beta, β_p , just before the disruption is plotted against the experimental current decay time, τ_{exp} . Blue symbols correspond to high β_p disruptive discharges, while red symbols represent the radiative disruptions with a massive neon gas-puff. Open squares represent the data analyzed in this study.

However, in JT-60U radiative disruptions, the plasma inductance and resistance varied with time. In particular, because the changing rate of plasma inductance was much larger than the time-averaged value of the resistance, it was suggested that the time derivative of plasma inductance (dL_p/dt) should be considered in the current decay model. The current decay time predicted by the modified L/R model, in which the time derivative of plasma inductance is considered, was introduced in Ref. [4] as

$$\tau_{L/(R+dL/dt)} = \frac{\bar{L}_p}{\Delta L_p/\Delta t + \bar{R}_p}, \quad (1)$$

where \bar{L}_p and \bar{R}_p are time-averaged values of L_p and R_p , respectively, and $\Delta L_p/\Delta t$ is the time derivative of plasma inductance during the initial phase of current quench. In fact, $\tau_{L/(R+dL/dt)}$ was in good agreement with the experimental current decay time.

High β plasma discharge is planned in ITER [5] and JT-60SA [6] to study the control of high β plasma for DEMO. In the high β plasma discharge, the generation of a large amount of bootstrap current is expected. However, the plasma discharges in Ref. [4] correspond to that of low β_p (poloidal beta) and mainly consist of ohmic current. Therefore, it is important to investigate the validation of the current decay model in high β_p plasmas. In this study, we investigated the validation of a current decay model in high β_p disruptive discharges in JT-60U through a comparative analysis with the time evolution of plasma resistance and inductance.

In Fig 1, β_p measured just before the thermal quench is plotted against the experimental current decay time, τ_{exp} ,

that is evaluated by using the following equation:

$$\tau_{exp} = I_{p0}/(\Delta I_p/\Delta t). \quad (2)$$

Here, I_{p0} is the plasma current just after the thermal collapse, ΔI_p is 10% of I_{p0} , and Δt is the time interval between I_{p0} and $0.9 \times I_{p0}$. In high β_p disruptive discharges, we focused on the initial phase of current quench in a similar manner as the analysis of the radiative disruption generated by a massive neon gas-puff [4]. β_p just before the thermal quench was evaluated from the measurement value of a magnetic sensor and an equilibrium calculation code (CCS code [7]). As indicated by Fig. 1, β_p values just before the disruption in high β_p disruptive discharges were above 1.4 and about 10 times larger than those in radiative disruptions. The plasma inductance, L_p , is evaluated from the following equation:

$$L_p = \mu_0 R_0 \left(\frac{l_i}{2} + \ln \frac{8R_0}{a} - 2 \right),$$

$$l_i = 2(\Lambda - \beta_p). \quad (3)$$

Here, Λ is Shafranov lambda, R_0 is major radius, and a is minor radius. As shown in Eq. (3), the assessment of β_p and Λ is important for obtaining the plasma inductance. Shafranov lambda was evaluated by using the measurement value of a magnetic sensor and the CCS code in JT-60U. Because the toroidal flux generated by eddy currents would strongly affect the evaluation of β_p by the measurement value of a magnetic sensor during the current quench phase, the β_p was assessed from the electron temperature evaluated by using ECE measurement and density evaluated by using a FIR interferometer. In this study, the time evolution of β_p was evaluated by the following equations:

$$\beta_p = \frac{p}{B_a^2/2\mu_0} = \alpha \frac{\int_0^a T_e(r)n_e r dr/S}{I_p^2/(4\pi^2 a^2)},$$

$$\alpha = \langle \beta_p \rangle / \langle \beta_p \rangle_{CCS}, \quad (4)$$

where $\langle \beta_p \rangle$ and $\langle \beta_p \rangle_{CCS}$ are the average values of β_p evaluated by Eq. (4) and CCS code just before the thermal quench, respectively, and S is the plasma cross section. In this analyzed data, the electron temperature profile can be evaluated in only five shots owing to the difficulty of measurement during disruptions. The data analyzed (five shots) in this study are represented by open squares in Fig. 1.

Next, we show the difference between high β_p disruptive discharges and radiative disruptions. Typical waveforms of plasma current, I_p , profile of electron temperature, T_e , plasma inductance, L_p , internal inductance, l_i , and poloidal beta, β_p , during disruption in high β_p disruptive discharges are shown in Fig. 2. The discharge was high β_p H-mode with the following magnetic configuration: elongation ratio, κ , = 1.58; triangularity, δ , = 0.18; and aspect ratio, ϵ , = 4.24. When the elongation ratio, κ is high,

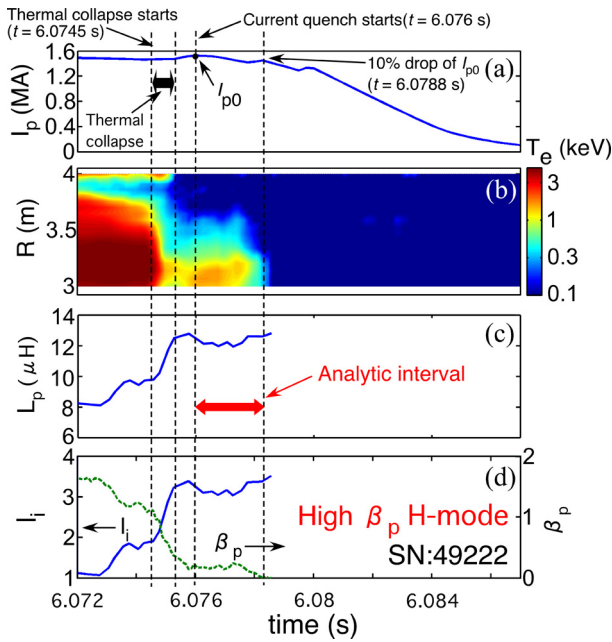


Fig. 2 Typical waveforms of (a) plasma current, (b) profile of electron temperature, (c) plasma inductance, and (d) internal inductance and poloidal beta in high β_p disruptions.

Eq. (3) is not applicable for estimating of L_p . For an elliptical cross-section, the equation of L_p is expressed as:

$$L_p = \mu_0 R_0 \left(\frac{l_i}{2} + \ln \frac{16R_0}{a(1+\kappa)} - 2 \right). \quad (5)$$

In high β_p disruptive discharges, we used Eq. (5) to estimate L_p because the elongation ratio of plasma before the disruption was 1.4-1.6 in all shots. In Fig. 2, the thermal collapse occurred at $t = 6.0745$ s. It should be noted that the thermal collapse means a rapid loss of the plasma energy in this study. After the thermal collapse began, the internal inductance increased, and plasma current increased slightly after the thermal collapse ended. The current quench started at $t = 6.076$ s, and the internal inductance gradually increased during the initial phase of current quench. The experimental current decay time was 18.9 ms, and the electron temperature at the plasma center was above 1 keV during the initial phase of current quench in this discharge.

On the other hand, in the radiative disruptions, the time evolution of l_i and T_e during disruption differed from those in the high β_p disruptive discharges. Figure 3 shows the time evolution of I_p , T_e , L_p , l_i , and β_p in the radiative disruptions. As shown in the figure, the thermal collapse occurred at $t = 16.3892$ s. After the thermal collapse began, the internal inductance decreased. Moreover, the plasma current increased during the same period; the plasma current increment in the density collapse cases was greater than that in the high β_p disruption cases. The current quench started at $t = 16.3905$ s, and the internal inductance gradually increased similar as the high β_p disrup-

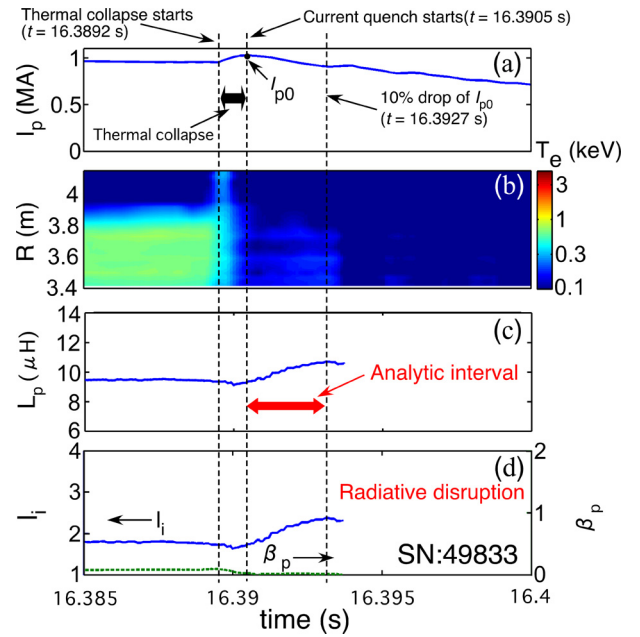


Fig. 3 Typical waveforms of (a) plasma current, (b) profile of electron temperature, (c) plasma inductance, and (d) internal inductance and poloidal beta in radiative disruptions with a massive neon gas-puff.

tions. The experimental current decay time was 19.2 ms, and the electron temperature at the plasma center was less than 0.5 keV. Although the experimental current decay times in Figs. 2 and 3 were almost the same, T_e at the plasma center in high β_p disruptive discharges was higher than twice of that in radiative disruptions.

In order to investigate the influence of electron temperature on the current decay time in high β_p and radiative disruptions, the electron temperature of the plasma center, T_{e0} , just after the thermal collapse, is plotted against τ_{exp} in Fig. 4. In high β_p disruptive discharges, T_{e0} was higher than 1 keV; in particular, T_{e0} in three shots exceeded 3 keV. In contrast, T_{e0} was less than 0.8 keV in radiative disruptions under the almost same current decay time observed in high β_p disruptions. Because the stored plasma energy was released by a massive neon gas-puff injection before the disruption, T_{e0} was lower in radiative disruptions. This experimental result indicates that the electron temperature itself plays no major role in determination of the current decay time in the initial phase of the disruption.

As discussed above, the plasma parameter during disruption in high β_p disruptive discharges differed completely from that in radiative disruptions with a massive neon gas-puff. In order to validate the current decay model in various discharges, we evaluated the experimental and predicted current decay times during the current quench in high β_p disruptive discharges. Figure 5 shows the predicted current decay time, τ_{model} , in high β_p disruptive discharges as a function of the experimental current decay time, τ_{exp} . The time evolution of R_p was evaluated from the T_e profile by the following equation:

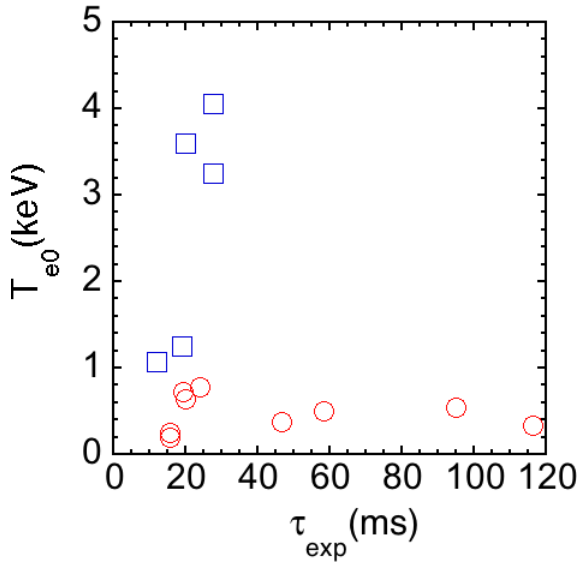


Fig. 4 The electron temperature of plasma center just after the thermal quench, T_{e0} , is plotted against the experimental current decay time, τ_{exp} . The electron temperature during disruption is evaluated by using ECE measurement. Blue squares correspond to high β_p disruptive discharges, while red circles indicate radiative disruptions with a massive neon gas-puff.

$$R_p = \frac{R_0}{\int_0^a \sigma_p(r) r dr},$$

$$\sigma_p(r) = \frac{1}{\eta_{\text{spitzer}}(r)} = \frac{T_e^{3/2}}{1.65 \times 10^{-9} Z_{\text{eff}} \ln \Lambda}, \quad (6)$$

where $\sigma_p(r)$ and $\eta_{\text{spitzer}}(r)$ are the local values of plasma conductivity and Spitzer resistivity [2], respectively, and Z_{eff} and $\ln \Lambda$ are the effective charge and Coulomb logarithm, respectively. In this estimation, we assumed an uniform Z_{eff} at three. In this figure, τ_{exp} was evaluated by using Eq. (2), and τ_{model} was evaluated by using both the conventional “ L/R model” ($\tau_{L/R}$) and the modified L/R model represented by Eq. (1) ($\tau_{L/(R+dL/dr)}$) in the initial phase of current quench. As shown in Fig. 5, the values of $\tau_{L/(R+dL/dr)}$ were in good agreement with those of τ_{exp} , while $\tau_{L/R}$ was two orders of magnitude larger than τ_{exp} in high β_p disruptive discharges. This result indicates that the effect of the time derivative of plasma inductance should be considered in the current decay model in high β_p disruptive discharges. The modified L/R model is available for both high β_p and radiative disruptions.

In summary, the validation of a current decay model during current quench was investigated in high β_p disruptive discharges in JT-60U. During the initial phase of current quench, the plasma resistance was estimated from the electron temperature profile measured using the ECE diagnostic system. The plasma inductance was calculated from Shafranov lambda evaluated by the CCS method, and the poloidal beta evaluated from electron temperature and density. It was experimentally confirmed that electron tem-

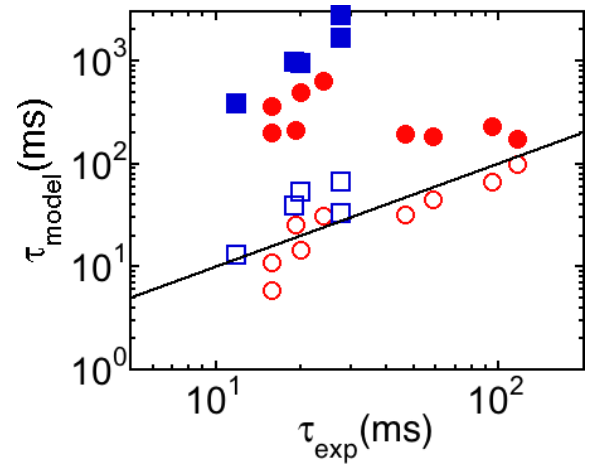


Fig. 5 Predicted current decay time, τ_{model} , in high β_p disruptive discharges and radiative disruptions with a massive neon gas-puff are plotted against the experimental current decay time. Close symbols were predicted by the conventional “ L/R model” ($\tau_{L/R}$) and open symbols were predicted by the “modified L/R model” considering dL_p/dt . Blue and red symbols represent high β_p disruptive discharges and radiative disruptions with a massive neon gas-puff, respectively.

perature does not play an important role in the determination of the current decay time in the initial phase of current quench and that values obtained from the L/R model are two orders of magnitude larger than the experimental results. The current decay time predicted by the “modified L/R model”, in which the time derivative of plasma inductance was considered, was in good agreement with the experimental data. In future work, we need to perform the MHD equilibrium code for free-boundary condition, such as DINA [8] and TSC [9] code, under an axisymmetric assumption to understand the determination mechanism of the time derivative of plasma inductance.

This work was supported by the JAEA collaborative research, collaborative research program of the NIFS, and Grant-in-Aid for Japan Society for the Promotion of Science (JSPS) Fellow.

- [1] T.C. Hender *et al.*, Progress in the ITER Physical Basis Chapter 3, Nucl. Fusion **47**, S128 (2007).
- [2] L. Spitzer and R. Härm, Phys. Rev. **89**, 977 (1953).
- [3] S.P. Gerhardt, J.E. Menard and the NSTX Team, Nucl. Fusion **49**, 025005 (2009).
- [4] Y. Shibata, K.Y. Watanabe, M. Okamoto, N. Ohno, A. Isayama *et al.*, Nucl. Fusion **50**, 025015 (2010).
- [5] M. Shimada *et al.*, Progress in the ITER Physical Basis Chapter 1, Nucl. Fusion **47**, S1 (2007).
- [6] S. Ishida, P. Barabaschi, Y. Kamada and the JT-60SA Team, Fusion Eng. Des. **85**, 2070 (2010).
- [7] K. Kurihara, Fusion Eng. Des. **51–52**, 1049 (2000).
- [8] R.R. Khayrutdinov and V.E. Lukash, J. Comput. Phys. **109**, 193 (1993).
- [9] S.C. Jardin, N. Pomphrey and J. Delucia, J. Comput. Phys. **66**, 481 (1986).